Role of SUMOylation of STAT1 in tubular epithelial-mesenchymal transition induced by high glucose

CUNYANG GU[1*], FENG GAO[2*], SHIQI ZHANG[1], LIHUA KANG[1], WEI ZHANG[1], XIAOJUAN FENG[1], JINXI LIU[1], YUEXIN TIAN[1], QUN WEI[3], YUNXIA DU[1], YUJIA XING[1], QINGJUAN LIU[1] and SHUXIA LIU[1]

[1]Department of Pathology, Hebei Medical University, Key Laboratory of Kidney Diseases of Hebei Province, Shijiazhuang, Hebei 050017; [2]Department of Pathology, The Third Affiliated Hospital of Hebei Medical University; [3]Department of Hospital Infection Control, Department of Public Health, Hebei General Hospital, Shijiazhuang, Hebei 050051, P.R. China

Received July 20, 2022; Accepted November 30, 2022

DOI: 10.3892/mmr.2023.12929

Abstract. Tubulointerstitial fibrosis (TIF) is an important pathological change that occurs during the development of diabetic kidney disease. The epithelial-mesenchymal transition (EMT) of renal tubular epithelial cells is a manifestation of TIF. STAT1, a member of the STAT family of transcription factors, can be modified by the small ubiquitin-related modifier (SUMO), thus affecting the activity of STAT1. The present study investigated the role of STAT1 SUMOylation in high glucose-induced tubular EMT by western blotting, immunocytochemistry, immunofluorescence, co-immunoprecipitation and dual luciferase reporter analysis. The results indicated that in the process of high glucose-induced EMT, STAT1 activation protected the cells from EMT. However, high glucose also increased the SUMOylation of STAT1, which prevented STAT1 from exerting an effective protective role by inhibiting its activity.

Introduction

According to the International Diabetes Federation, there will be 592 million patients with diabetes worldwide by 2035 (1). Diabetic kidney disease (DKD) is a complication that occurs in >20% of patients with diabetes (2) and it is the main cause of end-stage renal disease (ESRD) (3). The US Renal Data System 2020 Annual Data Report demonstrated that the percentage of patients with ESRD and diabetes mellitus increased form 58.3% in 2016 to a peak of 60.5% in 2019 before decreasing to 59.9% in 2020 (4). Furthermore, the increase in the percentage of patients with chronic kidney disease (CKD) caused by diabetes has shifted the spectrum of CKD in China toward its pattern in developed countries. These findings suggested there may be a rising incidence of diabetes-related ESRD in China (5). Tubulointerstitial fibrosis (TIF) is a common pathway in chronic kidney diseases, which eventually leads to ERSD. TIF is also a better predictor of kidney disease than glomerulosclerosis (6). TIF is characterized by deposition of the extracellular matrix, which is mainly produced by myofibroblasts. Renal proximal tubule epithelial cells, through epithelial-mesenchymal transition (EMT), are one of the main sources of myofibroblasts. Mounting evidence has revealed that interventions aimed at inhibiting EMT can significantly prevent DKD-induced renal fibrosis (7-9).

As a signal transduction and transcription activator, STAT is phosphorylated to form a dimer, which translocates to the nucleus to induce the transcription of target genes. Notably phosphorylated (p)-STAT is considered its active form. Studies have shown that p-STAT1 and p-STAT3 are involved in EMT and subsequent TIF under several conditions (10-13). The role of STAT3 in EMT and fibrosis has been widely recognized (14-18); however, other studies have suggested that the activation of STAT1 exhibits anti-fibrotic properties by reducing macrophage infiltration or changing the phenotype of macrophages in renal ischemia-reperfusion injury (19). Tumor-related studies have also demonstrated that the activation of STAT1 mediated the effect of interleukin-27 in reversing trophoblast cell EMT (20). In addition, STAT1 activation can mediate the protective effect of IFN-γ on DKD glomerulosclerosis (2,21,22).

STAT1 can be modified by small ubiquitin-related modifier (SUMO), which affects its activity (23,24). The human-derived SUMO family is comprised of four members: SUMO1, SUMO2, SUMO3 and SUMO4, each with distinct distributions and functions (25,26). However, the mechanism underlying STAT1 SUMOylation in DKD remains unclear. Therefore, the present study investigated the possible role of

Correspondence to: Professor Qingjuan Liu or Professor Shuxia Liu, Department of Pathology, Hebei Medical University, Key Laboratory of Kidney Diseases of Hebei Province, 361 East Zhongshan Road, Shijiazhuang, Hebei 050017, P.R. China
E-mail: liuqj246@163.com
E-mail: susanliu1976@163.com

*Contributed equally

Key words: renal tubular epithelial cells, epithelial-mesenchymal transition, high glucose, small ubiquitin-related modifier, STAT1

STAT1 activation and the role of STAT1 SUMOylation in high glucose-induced tubular EMT.

Materials and methods

Materials. The HK-2 human renal proximal tubule epithelial cell line was purchased from American Type Culture Collection. DMEM was purchased from Gibco; Thermo Fisher Scientific, Inc. FBS was purchased from ScienCell Research Laboratories, Inc. Mannitol was purchased from Shanghai Aladdin Biochemical Technology Co., Ltd. The CellTiter 96® AQueous One Solution Cell Proliferation Assay was purchased from Promega Corporation. The BCA Protein Assay Kit was obtained from Beijing Solarbio Science & Technology Co., Ltd. Lipofectamine® 3000 was obtained from Invitrogen; Thermo Fisher Scientific, Inc. RIPA lysis was purchased from Shanghai BestBio. BSA and ECL system were obtained from neoFroxx GmbH and Tiangen Biotech Co., Ltd., respectively. Anti-SUMO2/3 (cat. no. ab3742), SUMO4 (cat. no. ab126606), UBC9 (cat. no. ab75854), p-STAT1 (cat. no. ab30645), vimentin (cat. no. ab92547) and α-SMA (cat. no. ab124964) antibodies were purchased from Abcam. Anti-E-cadherin (cat. no. 20874-1-AP), protein inhibitor of activated STAT (PIAS)1 (cat. no. 23395-1-AP), PIAS3 (cat. no. 13486-1-AP), GFP (cat. no. 66002-1-lg) and anti-β-actin (cat. no. 66009-1-lg) antibodies were purchased from Proteintech Group, Ltd. Anti-SUMO1 antibody (cat. no. 4930) was purchased from Cell Signaling Technology, Inc. Rabbit anti-STAT1 antibody (cat. no. 10144-2-AP) was purchased from Proteintech Group, Ltd. and mouse anti-STAT1 antibody (cat. no. sc-464) was purchased from Santa Cruz Biotechnology, Inc. Anti-PIAS4 antibody (cat. no. AF5329) was purchased from Affinity Biosciences, Ltd. Protein A/G PLUS agarose (cat. no. sc-2003) and normal IgG antibodies (cat. no. sc-2005) were obtained from Santa Cruz Biotechnology, Inc. The dual luciferase reporter assay kit was purchased from Promega Corporation. STAT1, PIAS4 and UBC9 small interfering RNAs (siRNAs) and the negative control siRNA (cat. no. siN0000001-1-10) were purchased from Guangzhou RiboBio Co., Ltd. The siRNA sequences were as follows: UBC9 siRNA475, 5'-AGT GCGCTATCCCTGGAAA-3', UBC9 siRNA552, 5'-GGC CAGCTATCACCATCAA-3', UBC9 siRNA259, 5'-GGG AAGGAGGCTTGTTCAA-3', STAT1 siRNA1, 5'-CAT GCGGTTGAACCCTACA-3', STAT1 siRNA2, 5'-GCACGC TGCCAATGATGTT-3', STAT1 siRNA3, 5'-CTGGATATA TCAAGACTGA-3', and PIAS4 siRNA, 5'-UUAUUGGAG GGGUAGUAGCCC-3'. The STAT1-wild type (STAT1-WT), STAT1-K703R (STAT1-KR; SUMOylation site mutation), STAT1-Y701E (STAT1-YE; sustained activation) plasmids and the plasmid vector (pCMV3-C-GFPSpark) were obtained from Sino Biological, Inc. The accession number used to design the plasmids is NM_007315.3. STAT1-Luc plasmid was obtained from Genomeditech. The two-step immunohistochemical detection reagent test kit (cat. no. PV-9001), containing polymer helper and polyperoxidase-anti-rabbit IgG antibody, was purchased from OriGene Technologies, Inc. The fluorescent secondary antibody (cat. no. SA00013-4) and horseradish peroxidase-conjugated secondary antibodies (cat. nos. SA00001-1 and SA00001-2) were purchased from Proteintech Group, Ltd.

Cell culture and treatment. HK-2 cells were cultured in DMEM (normal glucose, 5.5 mmol/l) supplemented with 10% FBS at 37˚C in a 5% CO_2 incubator. Cells were exposed to 30 mmol/l glucose for 0, 12, 24 and 48 h at 37˚C. Mannitol was used as an osmotic control. Cells were treated with mannitol (30 mmol/l) in the same manner as high glucose. An inverted fluorescence microscope was used to observe cell morphology.

Cell viability assay. Cell viability was determined using the CellTiter 96 AQueous One Solution assay, according to the manufacturer's protocol. Briefly, HK-2 cells were seeded in 96-well plates. Following treatment with high glucose for 0, 24 and 48 h at 37˚C, cells were incubated with CellTiter 96 AQueous One Solution for 2 h at 37˚C. Finally, the absorbance of the reaction product was measured at 490 nm using a microplate reader.

Cell transfection. When cells reached 70% confluence, they were transfected using Lipofectamine® 3000 according to the manufacturer's protocol. For siRNA transfection, Lipofectamine 3000 reagent and siRNAs (2.5 μg) were incubated for 15 min at room temperature, and the mixture was then added to the cell medium. For plasmid transfection, Lipofectamine 3000 reagent, P3000 reagent and plasmids (3 μg) were incubated for 15 min. The empty plasmid was used as a negative control. The mixture was then added to the cell culture medium. After 8 h incubation with the mixture at 37˚C, the cells were cultured under normal condition for 40 h. The cells were then treated with 30 mmol/l glucose for 12, 24 and 48 h at 37˚C. The transfection efficiency of plasmids and siRNAs was confirmed by western blotting.

Western blotting. HK-2 cells were lysed with RIPA lysis buffer containing 0.4% protease inhibitor and 1% phosphatase inhibitor for 40 min and were then quantified using a BCA assay kit. Protein samples (30 μg per lane) were separated by SDS-PAGE on 10% gels and were then transferred to polyvinylidene fluoride membranes. Subsequently, the membranes were blocked with BSA for 2 h at 37˚C and incubated with primary antibodies (1:1,000) overnight at 4˚C. Thereafter, the membranes were incubated with horseradish peroxidase-conjugated secondary antibodies (1:5,000) for 2 h at 37˚C. Protein samples were detected using an ECL system. β-actin was used as an internal reference protein and relative protein expression levels were semi-quantified using a Gel-Pro analyzer 4.0 (Media Cybernetics, Inc.).

Immunocytochemistry and immunofluorescence. E-cadherin and α-SMA were detected by immunocytochemistry and SUMOs were detected by immunofluorescence. A sterile cover glass was placed on a six-well plate to culture the cells. For immunocytochemistry, cells (~50% confluence) were fixed with 4% paraformaldehyde for 30 min at room temperature. Following permeabilization with 0.1% Triton X-100 for 30 min at 37˚C, cells were incubated with 3% H_2O_2 at 37˚C for 30 min to remove endogenous peroxidase. Primary antibodies (E-cadherin: 1:200, α-SMA: 1:250) were then added and incubated overnight at 4˚C. Subsequently, the cells were incubated with polymer helper and polyperoxidase-anti-rabbit IgG antibody at 37˚C for 30 min. Finally, the cells were stained with

diaminobenzidine. A positive signal was observed using an Olympus light microscope (Olympus Corporation). With the exception that a fluorescent secondary antibody (1:200) was used at 37˚C for 30 min and observation was performed under a fluorescence microscope, the immunofluorescence procedure was similar to the immunocytochemistry procedure.

Co-immunoprecipitation (Co-IP). HK-2 cells were lysed with RIPA lysis buffer containing 0.4% protease inhibitor and 1% phosphatase inhibitor mixture for 40 min and proteins were then quantified using a BCA assay kit. The lysate (800 μl) was incubated with mouse STAT1 antibody (1:200) or IgG antibody (1:200) on a mixer for 24 h at 4˚C and then incubated with protein A/G beads (20 μl) on the mixer at 4˚C overnight. Subsequently, the samples were washed four times with IP washing buffer at 500 x g for 5 min at 4˚C. After adding bromophenol blue protein indicator buffer, the extracted protein was boiled at 100˚C for 7 min and the expression of SUMOs and PIASs were analyzed using western blotting.

Dual luciferase reporter analysis. Lipofectamine 3000 was used for plasmid transfection and the dual-luciferase reporter assay system was used for STAT1 activity detection. The STAT1-WT or STAT1-KR plasmids were co-transfected into cells with the STAT1-Luc plasmid, and each group was simultaneously transfected with the *Renilla* luciferase plasmid to eliminate the difference caused by different efficiencies. A total of 48 h after transfection, glucose (30 mmol/l) was added to the cells for 24 h. Subsequently, the dual luciferase reporter assay system was used to detect STAT1 activity. Briefly, the cells were lysed with PLB lysis buffer at room temperature. First, the LARII reagent was added to the lysate to detect firefly luciferase activity, and the Stop & Glo reagent was then added to detect the *Renilla* luciferase activity. STAT1 activity was expressed as the ratio of firefly luciferase activity to *Renilla* luciferase activity.

Statistical analysis. Each experiment was repeated at least three times. Statistical analyses were conducted using SPSS 19.0 statistical software (IBM Corporation). The measured data are expressed as the mean ± standard deviation. Normally distributed quantitative data were compared between two groups using independent-samples Student's t-test and data among multiple groups were compared using one-way ANOVA (with LSD or Tukey's test) or two-way ANOVA (with Bonferroni test). $P<0.05$ was considered to indicate a statistically significant difference.

Results

Effects of high glucose on cell viability and the phenotypic transition of HK-2 cells. The CellTiter 96 AQueous One Solution assay was used to determine the viability of HK-2 cells. The results revealed that high glucose did not affect cell viability (Fig. 1A). Under an inverted fluorescence microscope, most HK-2 cells were arranged in a typical cobblestone-like pattern when cultured with normal glucose, whereas the cells were elongated and exhibited a spindle-shaped morphology after 48 h of high-glucose treatment (Fig. 1B). Immunocytochemical analysis showed weak expression of E-cadherin and strong expression of α-SMA in the cytoplasm of HK-2 cells following high glucose treatment for 48 h (Fig. 1C). In addition, western blotting was used to detect the phenotypic transition of HK-2 cells (Fig. 1D and E). Among the three treatment groups, only high glucose increased the expression of vimentin and α-SMA, and decreased E-cadherin expression in a time-dependent manner. Compared with in the normal glucose treatment group, the expression levels of vimentin were significantly increased when cells were stimulated with high glucose for 24 h. In addition, α-SMA expression was significantly increased after 12 h of high-glucose stimulation. By contrast, the expression levels of E-cadherin were significantly downregulated after 12 h of high-glucose exposure and gradually decreased. These results indicated that high glucose may promote the EMT of HK-2 cells.

Effects of high glucose on SUMO expression in HK-2 cells. To investigate the effects of high glucose on the expression levels of SUMOs in HK-2 cells, immunofluorescence analysis (Fig. 2A) and western blotting (Fig. 2B and C) were performed. SUMOs were primarily expressed in the nucleus. Among the three treatment groups, only high glucose increased the expression levels of SUMO1 and SUMO4. As for SUMO2/3, although there was no marked change observed by immunocytochemistry, the western blotting results indicated that high glucose elevated the expression levels of SUMO2/3. Compared with in cells treated with normal glucose, the relative expression levels of SUMO1 and SUMO4 peaked 12 h after high-glucose treatment, whereas the relative expression levels of SUMO2/3 peaked at 24 h and then decreased.

Effects of STAT1 activation on the phenotypic transition in HK-2 cells. The present study observed the effect of high glucose on the phosphorylation of STAT1 (Fig. 3A and B). The results suggested that high glucose, but not normal glucose or mannitol, increased the relative expression levels of p-STAT1 (Tyr701) in a time-dependent manner.

To determine the role of STAT1 activation in tubular EMT induced by high glucose, STAT1 siRNA or STAT1-YE plasmids were transfected into the HK-2 cells. The transfection efficiency of siRNA and plasmids are presented in Fig. 3C-E. All three siRNAs inhibited STAT1 expression and STAT1 siRNA3, which had the best inhibitory effect, was selected for subsequent experiments (Fig. 3C and D). The fusion expression of GPF and STAT1 resulted in the molecular weight of exogenous STAT1 being higher than that of endogenous STAT1. The efficiency of transfection with the STAT1 plasmid was confirmed by detecting the expression of GFP-STAT1 (Fig. 3E). As shown in Fig. 3F and G, STAT1 siRNA transfection did not significantly affect the level of p-STAT1/STAT1 compared with control siRNA transfection; however, STAT1 siRNA transfection aggravated the effect of high glucose on the expression level of α-SMA. This may be due to the decreased level of STAT1. In order to verify that p-STAT1 affected high glucose-induced EMT, STAT1-YE plasmid was transfected into cells. The results showed that the expression levels of p-STAT1 were higher in the STAT1-YE group compared with those in the STAT1-WT group. The upregulation of STAT1 phosphorylation in the STAT1-YE group may alleviate the high glucose-induced changes in the

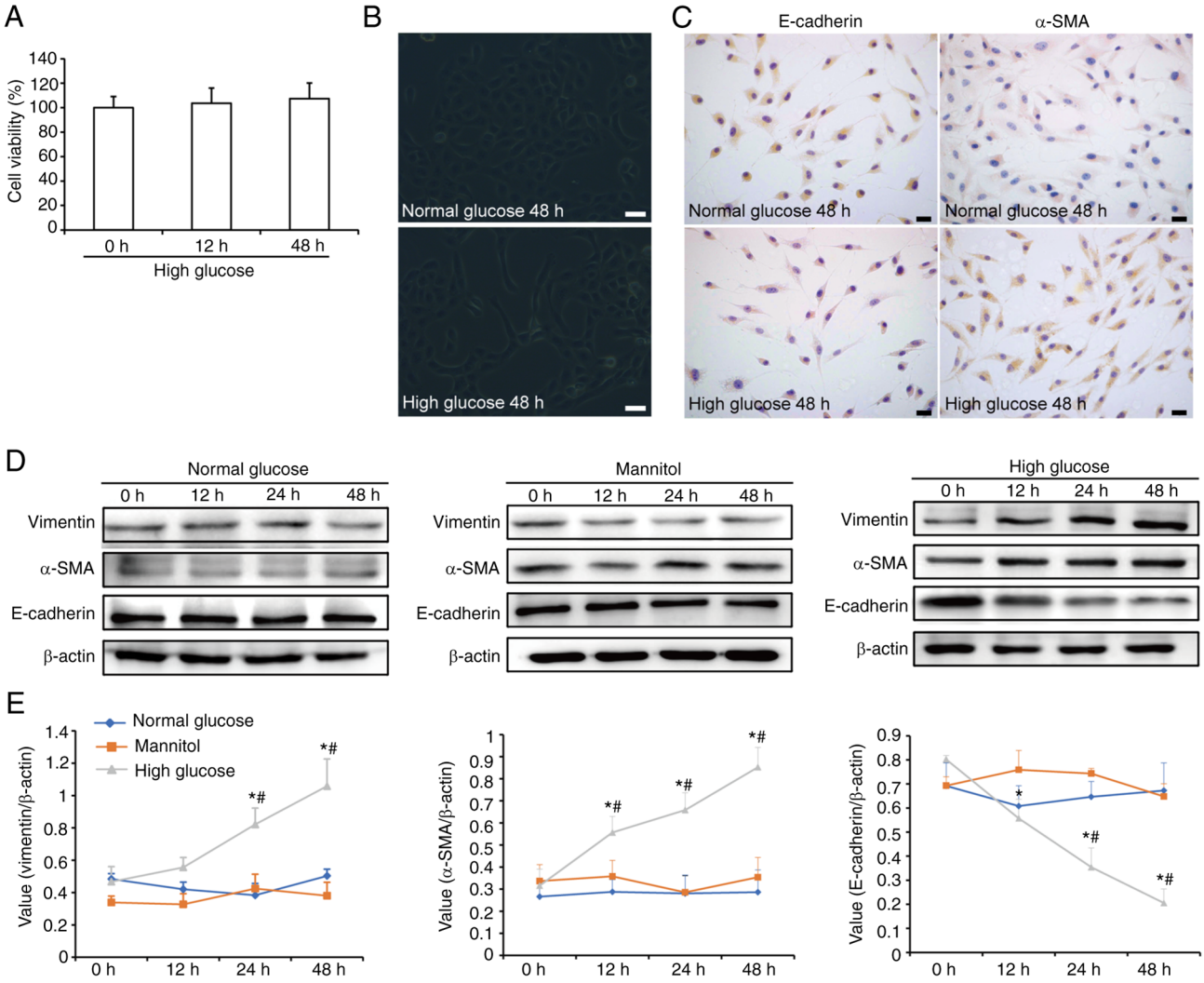

Figure 1. Effects of high glucose on the viability and phenotypic transition of HK-2 cells. (A) Cell viability was analyzed with the MTS assay. High glucose did not affect cellular viability. Data were analyzed by one-way ANOVA and LSD post hoc test. (B) Cell morphology was altered following high-glucose stimulation. The cells were elongated and exhibited a spindle-shaped morphology after 48 h of high-glucose treatment. Scale bars: 30 μm. (C) Immunocytochemistry was used to detect the expression levels of E-cadherin and α-SMA. The cells exhibited weak expression of E-cadherin and strong expression of α-SMA in the cytoplasm following high-glucose treatment for 48 h. Scale bars: 20 μm. Expression levels of vimentin, α-SMA and E-cadherin (D) were detected using western blotting and (E) were semi-quantified using densitometry. Compared with in the normal glucose treatment group, high glucose, but not mannitol, increased the expression levels of vimentin and α-SMA, and decreased E-cadherin expression. The data were analyzed by two-way ANOVA and Bonferroni post hoc test. n=3. *P<0.05 vs. 0 h; $^{\#}$P<0.05 vs. normal glucose group.

expression levels of E-cadherin and α-SMA (Fig. 3H and 3I). These results suggested that STAT1 activation may inhibit EMT in HK-2 cells.

SUMOylation of STAT1 in HK-2 cells. It has been reported that STAT1 can be modified using SUMOs. As UBC9 is the only E2 enzyme involved in SUMOylation, the present study first verified the conjunction of STAT1 and UBC9. As shown in Fig. 4A, there was enhanced conjunction of STAT1 and UBC9 under high glucose conditions. Subsequently, the binding of STAT1 and SUMOs in UBC9 siRNA-transfected cells was detected. All three siRNAs inhibited UBC9 expression (Fig. 4B); UBC9-si475 exhibited the best inhibitory effect and was selected for subsequent experiments. As shown in Fig. 4C and D, high glucose levels upregulated the binding of STAT1 with all three SUMOs, which could be inhibited by UBC9 knockdown. This indicated that STAT1 could be modified by SUMOs in HK-2 cells. SUMOylation of STAT1 was enhanced under high glucose conditions. Subsequently, it was confirmed by co-IP experiments that the binding of PIAS4, instead of PIAS1 or PIAS3, to STAT1 was increased under high glucose conditions. These findings suggested that PIAS4 may be the E3 ligase which mediated the upregulation of STAT1 SUMOylation (Fig. 4E). Subsequently, HK-2 cells were transfected with PIAS4 siRNA (Fig. 4F). The results revealed that the binding of SUMO1 and SUMO4 with STAT1 was inhibited after PIAS4 was knocked down (Fig 4G and H). The slight bands seen in Fig. 4A and E may be caused by the light or heavy chains of IgG, respectively. In addition, the slight bands seen in Fig. 4G may be due to insufficient cleaning in the experiments.

Effects of STAT1 SUMOylation on its activity. In order to verify the effect of STAT1 SUMOylation on its activity, the STAT1-KR plasmid was generated. In STAT1-KR,

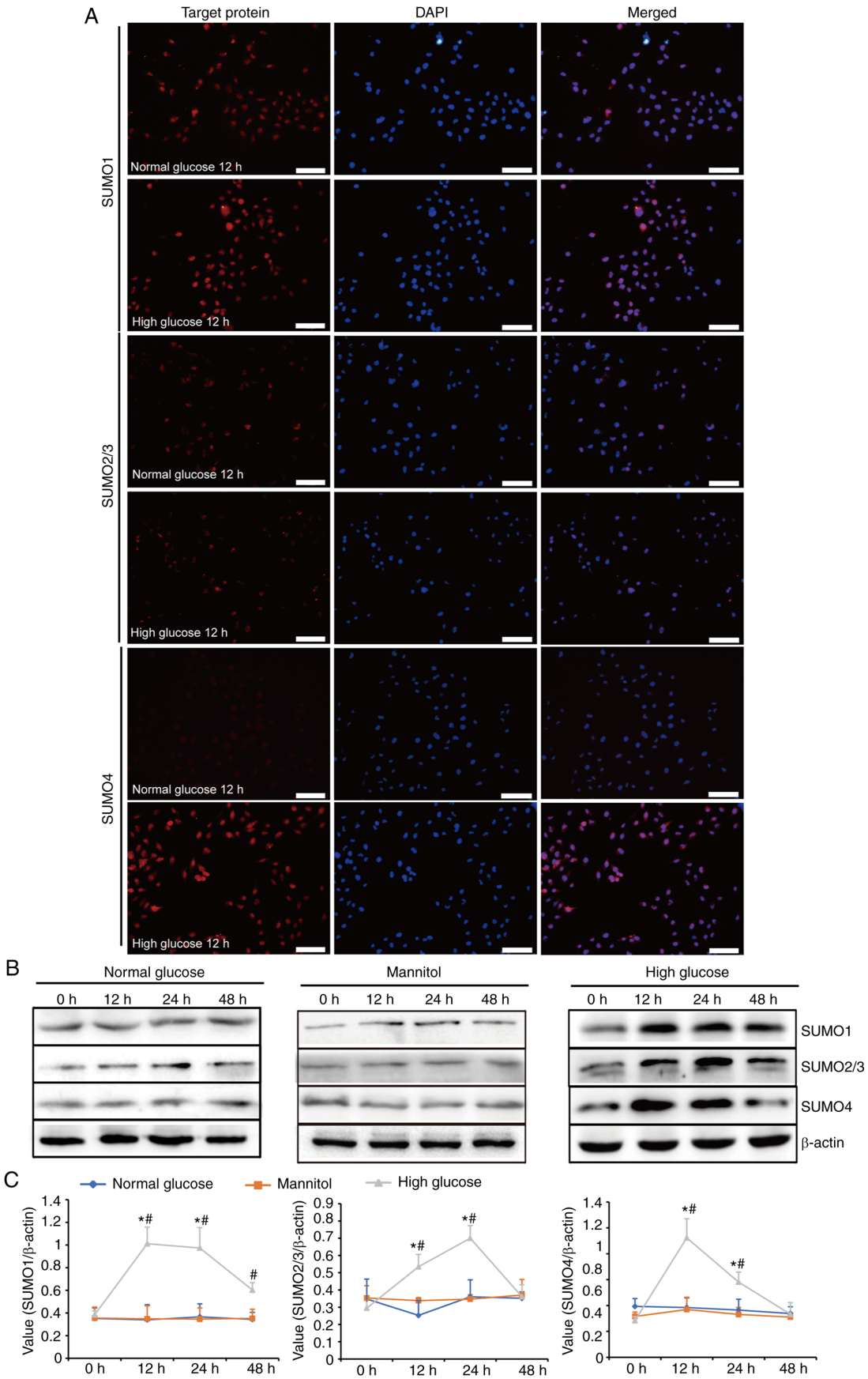

Figure 2. High glucose increases the expression levels of SUMOs in HK-2 cells. (A) Immunofluorescence was used to detect SUMO expression. SUMOs were primarily expressed in the nucleus. After 12 h high-glucose stimulation, the expression levels of SUMO1 and SUMO4 increased, whereas the fluorescence signal of SUMO2/3 did not change. SUMO expression levels (B) were detected using western blotting and (C) were semi-quantified using densitometry. Compared with in the normal glucose treatment group, high glucose, but not mannitol, increased the expression levels of all SUMOs. The data were analyzed by two-way ANOVA and Bonferroni post hoc test. n=3. Scale bars: 100 μm. *P<0.05 vs. 0 h; $^{\#}$P<0.05 vs. normal glucose group. SUMO, small ubiquitin-related modifier.

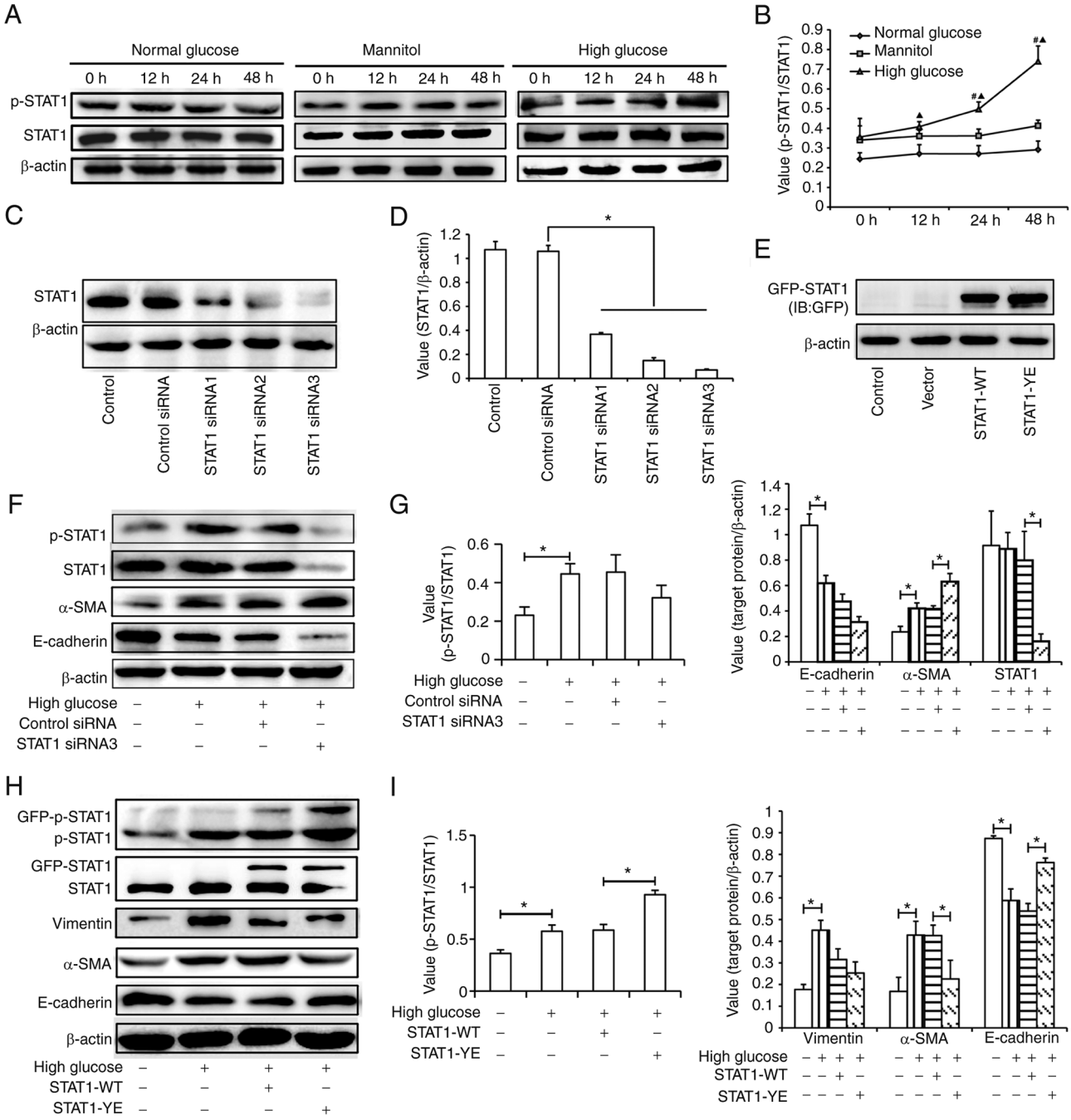

Figure 3. STAT1 activation inhibits phenotypic transition of HK-2 cells. The activation of STAT1 (A) was detected using western blotting and (B) was semi-quantified using densitometry. High glucose increased the relative expression levels of p-STAT1 (Tyr701). The data were analyzed by two-way ANOVA and Bonferroni post hoc test. The efficiency of STAT1 knockdown (C) was analyzed by western blotting and (D) was semi-quantified using densitometry. The data were analyzed by one-way ANOVA and Tukey post hoc test. (E) Efficiency of plasmids transfection. The expression of p-STAT1, E-cadherin and α-SMA post-transfection with STAT1 siRNA (F) was detected using western blotting and (G) was semi-quantified using densitometry. The reduction in p-STAT1 aggravated the effects of high glucose on the expression levels of E-cadherin and α-SMA. The data were analyzed by one-way ANOVA and Tukey post hoc test. The expression of p-STAT1, E-cadherin, vimentin and α-SMA post-transfection with STAT1-WT or STAT1-YE plasmid (H) was detected using western blotting and (I) was semi-quantified using densitometry. Upregulation of STAT1 phosphorylation alleviated the high glucose-induced expression levels of E-cadherin, α-SMA and vimentin. The data were analyzed by one-way ANOVA and Tukey post hoc test. n=3. *P<0.05; #P<0.05 vs. 0 h; ▲P<0.05 vs. normal glucose group. p-, phosphorylated; siRNA, small interfering RNA; WT, wild type.

Lys 703 was mutated to Arg; this mutation can inhibit the SUMOylation of STAT1 at Lys 703. It has previously been suggested that the SUMOylation of STAT1 at Lys 703 affects the phosphorylation of STAT1 at Tyr701 (27). Fig. 5A shows the expression of GFP-STAT1, which confirmed the transfection efficiency of the STAT1 plasmids. As shown in Fig. 5B, high glucose induced the phosphorylation of exogenous STAT1 both in STAT1-WT and STAT1-KR groups. Compared with the STAT1-WT plasmid group, the level of total p-STAT1 was higher in the STAT1-KR plasmid group (Fig. 5B and C). Dual-luciferase reporter gene analysis suggested that high glucose significantly increased STAT1 activity; however, STAT1 was more active in the STAT1-KR plasmid group than that in the STAT1-WT plasmid group (Fig. 5D). These results

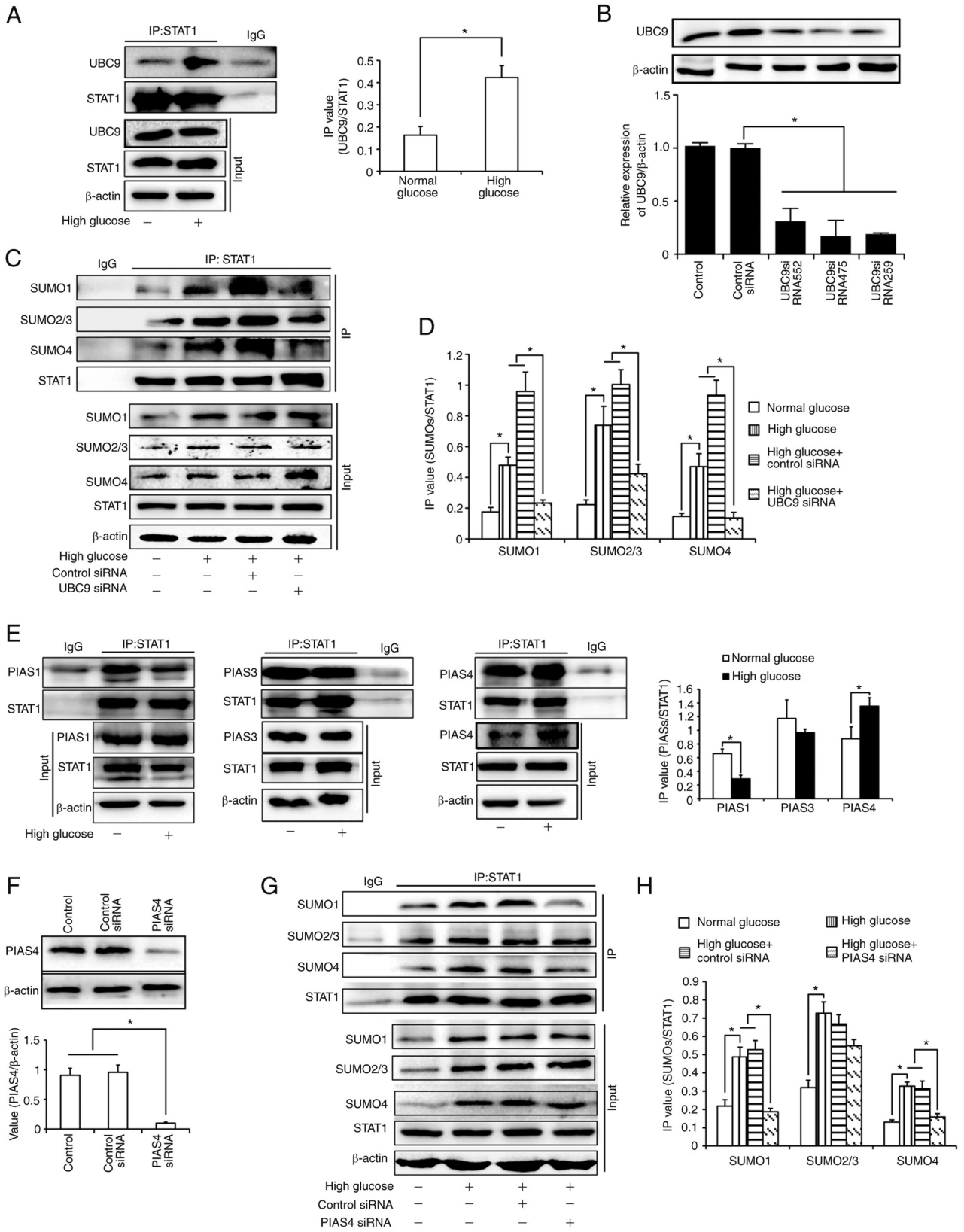

Figure 4. High glucose upregulates STAT1 SUMOylation in HK-2 cells. (A) Co-IP suggested that the binding of STAT1 and UBC9 was upregulated under high-glucose conditions. The data were analyzed by Student's t-test. (B) Efficiency of UBC9 knockdown was analyzed by western blotting and was semi-quantified using densitometry. The data were analyzed by one-way ANOVA and Tukey post hoc test. (C and D) Co-IP suggested that the SUMOylation of STAT1 was enhanced under high-glucose conditions. The data were analyzed by one-way ANOVA and Tukey post hoc test. (E) Binding of STAT1 and PIASs was analyzed. Results suggested that PIAS4 mediated the upregulation of STAT1 SUMOylation. The data were analyzed by Student's t-test. (F) Efficiency of PIAS4 knockdown was analyzed by western blotting and was semi-quantified using densitometry. The data were analyzed by one-way ANOVA and LSD post hoc test. The effects of PIAS4 siRNA transfection on STAT1 SUMOylation (G) were analyzed by co-IP and (H) were semi-quantified using densitometry. The results suggested that PIAS4 knockdown inhibited STAT1 SUMOylation. The data were analyzed by one-way ANOVA and Tukey post hoc test. IP:STAT1 means the cell lysate was incubated with STAT1 antibody. Input was used as a positive control to detect the presence of target proteins. n=3. *P<0.05. Co-IP, co-immunoprecipitation; PIAS, protein inhibitor of activated STAT; siRNA, small interfering RNA; SUMO, small ubiquitin-related modifier.

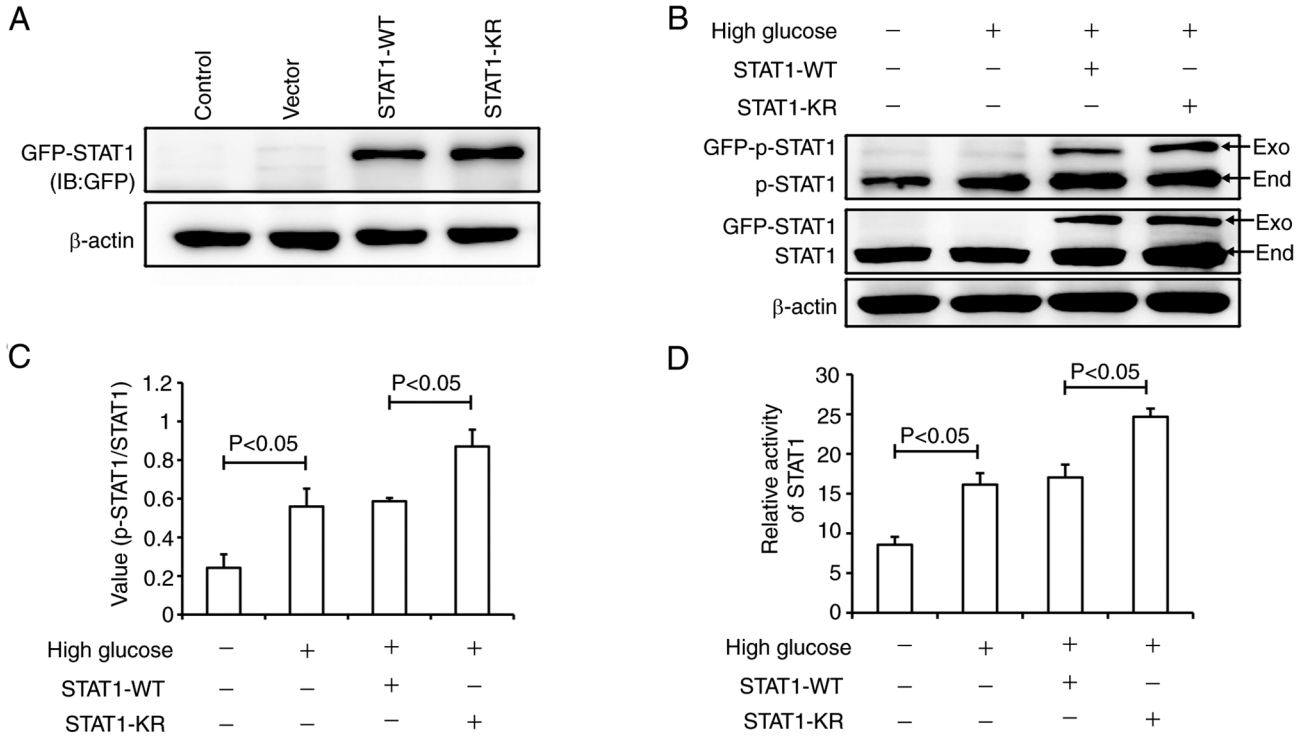

Figure 5. Inhibition of STAT1 SUMOylation upregulates STAT1 activity induced by high glucose. (A) Transfection efficiency of STAT1-WT and STAT1-YE plasmids was detected by western blotting. The expression level of p-STAT1 (B) was detected using western blotting and (C) was semi-quantified using densitometry. Compared with in the STAT1-WT plasmid group, the level of p-STAT1 was higher in the STAT1-KR plasmid group. (D) Dual luciferase reporter assay suggested that STAT1 activity was increased in STAT1-KR plasmid group. All of the data were analyzed by one-way ANOVA and Tukey post hoc test. n=3. p-, phosphorylated; WT, wild type; Exo, exogenous STAT1; End, endogenous STAT1

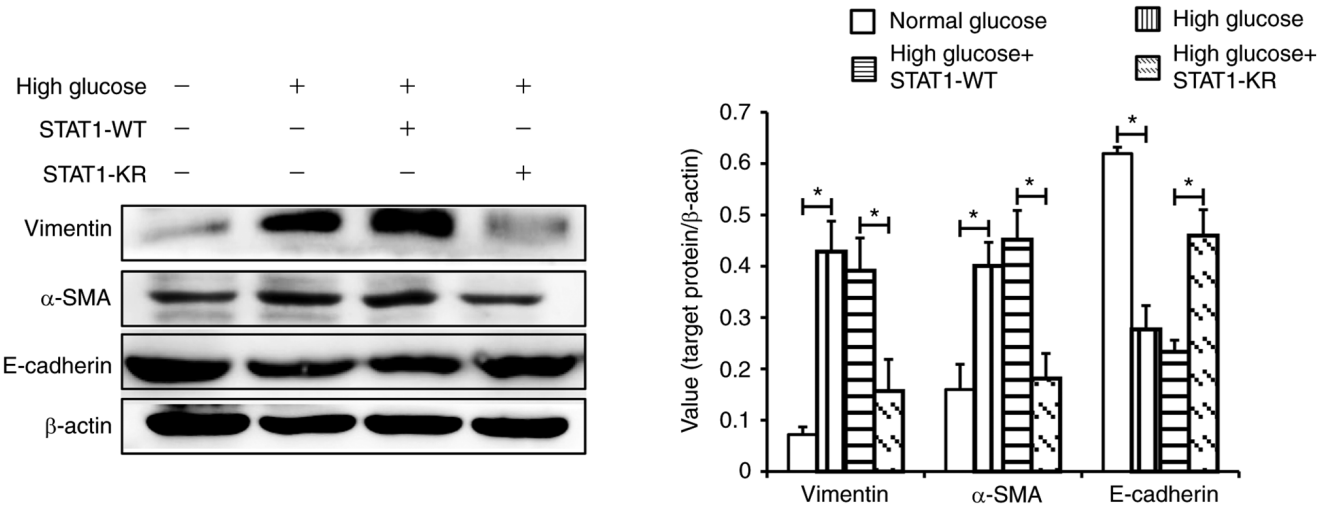

Figure 6. Inhibition of STAT1 SUMOylation improves the phenotypic transition of HK-2 cells induced by high glucose. Expression levels of vimentin, α-SMA and E-cadherin were detected using western blotting and were semi-quantified using densitometry. The results suggested that activated STAT1 suppresses the high glucose-induced phenotypic transition of HK-2 cells. The data were analyzed by one-way ANOVA and Tukey post hoc test. n=3. *P<0.05. WT, wild type.

suggested that STAT1-KR transfection increased p-STAT1 expression and STAT1 activity.

Role of STAT1 SUMOylation in the phenotypic transition of HK-2 cells. As shown in Fig. 6, under high glucose, E-cadherin expression was higher, and α-SMA and vimentin expression was lower in the STAT1-KR plasmid group compared with that in the STAT1-WT plasmid group. These results suggested that activated STAT1 may suppress the high glucose-induced phenotypic transition of HK-2 cells.

Discussion

DKD is one of the most common microvascular complications associated with diabetes. The major pathological changes in DKD include glomerulosclerosis and TIF. Although

glomerulopathy was originally considered the main pathological change in DKD, there is increasing evidence that TIF is more closely related to renal function. TIF can be detected in the early stages of DKD and directly contributes to decreased renal function, independent of glomerular dysfunction (10,28). Myofibroblasts are the main cells that produce the extracellular matrix, leading to TIF, and EMT in renal tubular epithelial cells is a key source of myofibroblasts (29,30). EMT is characterized by the loss of epithelial adhesion molecules and the expression of myofibroblast markers in the renal tubular epithelial cells (31,32). In the present study, HK-2 cells were stimulated with 30 mmol/l glucose. The subsequent decrease in E-cadherin, and the increase in α-SMA and vimentin confirmed that high glucose induced tubular EMT.

Given the uncertainty regarding the role of STAT1 activation in EMT and fibrosis, STAT1 siRNA was transfected into HK-2 cells to explore the possible role of STAT1 in tubular EMT. The results revealed that STAT1 knockdown aggravated the effects of high glucose on the expression levels of α-SMA in HK-2 cells. As unphosphorylated STAT1 also induces the expression of some genes (33), and STAT1 siRNA reduced the expression levels of STAT1 rather than p-STAT1/STAT1, it may be suggested that the effect of STAT1 siRNA transfection on the expression of α-SMA could be due to the decreased levels of STAT1. The present study transfected the cells with the STAT1-YE plasmid to verify the role of STAT1 activation in tubular EMT. The levels of p-STAT1 were higher in the STAT1-YE group than in the STAT1-WT group and the increased STAT1 phosphorylation exhibited an inhibitory effect on EMT. Therefore, it was suggested that activated STAT1 may play a protective role in EMT. Similar results demonstrated a protective effect of STAT1 against renal fibrosis. For example, in a previous study, $STAT1^{-/-}$ mice exhibited higher amounts of α-SMA, glomerular density, and Masson's trichrome, silver, and collagen staining (19). IFN-γ can activate STAT1 to suppress the overexpression of TGF-β, collagen IV and connective tissue growth factor in diabetic mice and in high glucose-stimulated mesangial cells (22). In addition, p-STAT1 mediates the inhibitory role of IL-27 in EMT of trophoblast cells (20). These results suggest a protective role for STAT1 in EMT or fibrosis.

The activity of STAT1 is regulated by several factors, and SUMOylation can affect its phosphorylation (24). STAT1 harbors a functional SUMOylation consensus sequence, ΨKXE, where Ψ represents a large hydrophobic residue, K represents lysine, X represents any amino acid and E represents glutamate (34). The present study demonstrated that STAT1 could be modified by SUMOs in HK-2 cells and that SUMOylation of STAT1 was enhanced under high-glucose conditions. To identify the effect and mechanism of STAT1 SUMOylation on high glucose-induced EMT, STAT1-WT and STAT1-KR plasmids were transfected into HK-2 cells. The results revealed that high glucose weakly induced E-cadherin, vimentin and α-SMA expression in STAT1-KR plasmid-transfected cells compared with in STAT1-WT plasmid-transfected cells. In other words, inhibition of STAT1 SUMOylation reduced EMT. In addition, the p-STAT1 expression levels in cells transfected with STAT1-KR plasmids were higher than those in the STAT1-WT plasmid-transfected cells. The results of dual-luciferase reporter gene analysis showed that the transcriptional activity of STAT1 was significantly upregulated in cells transfected with STAT1-KR plasmid compared with in those transfected with STAT1-WT plasmid. Although p-STAT1 has been reported to perform specific functions in the cytoplasm (35), the present results suggested that the upregulation of STAT1 SUMOylation may affect tubular EMT by inhibiting the activity of STAT1 under high-glucose conditions.

In conclusion, the upregulation of STAT1 SUMOylation caused by high glucose levels may explain why STAT1 could not be effectively activated to exert its protective effect. However, how SUMOylation affects the activity of STAT1 and the genes that mediate the effect of STAT1 activity on EMT requires further study.

Acknowledgements

Not applicable.

Funding

This study was supported by the National Natural Science Foundation (grant nos. 81600564, 81800623 and 21605035), the Hebei Natural Science Foundation (grant nos. H2020206262 and H2019206045), and the Department of Health of Hebei Province (grant no. 20180044).

Availability of data and materials

The datasets used and/or analyzed during the current study are available from the corresponding author on reasonable request.

Authors' contributions

QL and SL are responsible for conceiving and designing the research. CG, LK, SZ, JL and YX are responsible for performing the experiments. FG, WZ and QW are responsible for analyzing data. XF, YD and YT are responsible for interpreting the results of experiments and editing manuscript QL and CG confirm the authenticity of all the raw data. All authors read and approved the final manuscript.

Ethics approval and consent to participate

Not applicable.

Patient consent for publication

Not applicable.

Competing interests

The authors declare that they have no competing interests.

References

1. Shi Y and Hu FB: The global implications of diabetes and cancer. Lancet 383: 1947-1948, 2014.
2. Murphy D, McCulloch CE, Lin F, Banerjee T, Bragg-Gresham JL, Eberhardt MS, Morgenstern H, Pavkov ME, Saran R, Powe NR, *et al*: Trends in prevalence of chronic kidney disease in the United States. Ann Intern Med 165: 473-481, 2016.

3. Rossing P: Diabetic nephropathy: Worldwide epidemic and effects of current treatment on natural history. Curr Diab Rep 6: 479-483, 2006.
4. Johansen KL, Chertow GM, Foley RN, Gilbertson DT, Herzog CA, Ishani A, Israni AK, Ku E, Tamura MK, Li S, *et al*: US renal data system 2020 annual data report: Epidemiology of kidney disease in the United States. Am J kidney Dis 77: A7-A8, 2021.
5. Yang C, Wang H, Zhao X, Matsushita K, Coresh J, Zhang L and Zhao MH: CKD in China: Evolving spectrum and public health implications. Am J Kidney Dis 76: 258-264, 2020.
6. Nauta FL, Boertien WE, Bakker SJ, van Goor H, van Oeveren W, de Jong PE, Bilo H and Gansevoort RT: Glomerular and tubular damage markers are elevated in patients with diabetes. Diabetes Care 34: 975-981, 2011.
7. Du L, Qian X, Li Y, Li XZ, He LL, Xu L, Liu YQ, Li CC, Ma P, Shu FL, *et al*: Sirt1 inhibits renal tubular cell epithelial-mesenchymal transition through YY1 deacetylation in diabetic nephropathy. Acta Pharmacol Sin 42: 242-251, 2020.
8. Yang T, Shu F, Yang H, Heng C, Zhou Y, Chen Y, Qian X, Du L, Zhu X, Lu Q and Yin X: YY1: A novel therapeutic target for diabetic nephropathy orchestrated renal fibrosis. Metabolism 96: 33-45, 2019.
9. Yang T, Heng C, Zhou Y, Hu Y, Chen S, Wang H, Yang H, Jiang Z, Qian S, Wang Y, *et al*: Targeting mammalian serine/threonine-protein kinase 4 through Yes-associated protein/TEA domain transcription factor-mediated epithelial-mesenchymal transition ameliorates diabetic nephropathy orchestrated renal fibrosis. Metabolism 108: 154258, 2020.
10. Huang F, Zhao Y, Wang Q, Hillebrands JL, van den Born J, Ji L, An T and Qin G: Dapagliflozin attenuates renal tubulointerstitial fibrosis associated with type 1 diabetes by regulating STAT1/TGFβ1 signaling. Front Endocrinol (Lausanne) 10: 441, 2019.
11. Li Y, Zhou H, Li Y, Han L, Song M, Chen F, Shang G, Wang D, Wang Z, Zhang W and Zhong M: PTPN2 improved renal injury and fibrosis by suppressing STAT-induced inflammation in early diabetic nephropathy. J Cell Mol Med 23: 4179-4195, 2019.
12. Luan J, Fu J, Wang D, Jiao C, Cui X, Chen C, Liu D, Zhang Y, Wang Y, Yuen PST, *et al*: MiR-150-based RNA interference attenuates tubulointerstitial fibrosis through the SOCS1/JAK/STAT pathway in vivo and in vitro. Mol Ther Nucleic Acids 22: 871-884, 2020.
13. Zhao SQ, Shen ZC, Gao BF and Han P: microRNA-206 overexpression inhibits epithelial-mesenchymal transition and glomerulosclerosis in rats with chronic kidney disease by inhibiting JAK/STAT signaling pathway. J Cell Biochem 120: 14604-14617, 2019.
14. Zhang X, Lu H, Xie S, Wu C, Guo Y, Xiao Y, Zheng S, Zhu H, Zhang Y and Bai Y: Resveratrol suppresses the myofibroblastic phenotype and fibrosis formation in kidneys via proliferation-related signalling pathways. Br J Pharmacol 176: 4745-4759, 2019.
15. Li X, Zhang F, Qu L, Xie Y, Ruan Y, Guo Z, Mao Y, Zou Q, Shi M, Xiao Y, *et al*: Identification of YAP1 as a novel downstream effector of the FGF2/STAT3 pathway in the pathogenesis of renal tubulointerstitial fibrosis. J Cell Physiol 236: 7655-7671, 2021.
16. Liu J, Zhong Y, Liu G, Zhang X, Xiao B, Huang S, Liu H and He L: Role of Stat3 signaling in control of EMT of tubular epithelial cells during renal fibrosis. Cell Physiol Biochem 42: 2552-2558, 2017.
17. Zhang Y, Zou J, Tolbert E, Zhao TC, Bayliss G and Zhuang S: Identification of histone deacetylase 8 as a novel therapeutic target for renal fibrosis. FASEB J 34: 7295-7310, 2020.
18. Shi Y, Tao M, Ma X, Hu Y, Huang G, Qiu A, Zhuang S and Liu N: Delayed treatment with an autophagy inhibitor 3-MA alleviates the progression of hyperuricemic nephropathy. Cell Death Dis 11: 467, 2020.
19. Kemmner S, Bachmann Q, Steiger S, Lorenz G, Honarpisheh M, Foresto-Neto O, Wang S, Carbajo-Lozoya J, Alt V, Schulte C, *et al*: STAT1 regulates macrophage number and phenotype and prevents renal fibrosis after ischemia-reperfusion injury. Am J Renal Physiol 316: F277-F291, 2019.
20. Ge H, Yin N, Han TL, Huang D, Chen X, Xu P, He C, Tong C and Qi H: Interleukin-27 inhibits trophoblast cell invasion and migration by affecting the epithelial-mesenchymal transition in preeclampsia. Reprod Sci 26: 928-938, 2019.
21. Du J, Dong W, Li H, Li B, Liu X, Kong Q, Sun W, Sun T, Ma P, Cui Y and Kang P: Protective effects of IFN-γ on the kidney of type-2 diabetic KKAy mice. Pharmacol Rep 70: 607-613, 2018.
22. Du J, Wang L, Liu L, Fan Q, Yao L, Cui Y, Kang P, Zhao H, Feng X and Gao H: IFN-γ suppresses the high glucose-induced increase in TGF-β1 and CTGF synthesis in mesangial cells. Pharmacol Rep 63: 1137-1144, 2011.
23. Maarifi G, Maroui MA, Dutrieux J, Dianoux L, Nisole S and Chelbi-Alix MK: Small ubiquitin-like modifier alters IFN response. J Immunol 195: 2312-2324, 2015.
24. Sampaio EP, Ding L, Rose SR, Cruz P, Hsu AP, Kashyap A, Rosen LB, Smelkinson M, Tavella TA, Ferre EMN, *et al*: Novel signal transducer and activator of transcription 1 mutation disrupts small ubiquitin-related modifier conjugation causing gain of function. J Allergy Clin Immunol 141: 1844-1853 e1842, 2018.
25. Johnson ES: Protein modification by SUMO. Annu Rev Biochem 73: 355-382, 2004.
26. Chang HM and Yeh ETH: SUMO: From bench to bedside. Physiol Rev 100: 1599-1619, 2020.
27. Begitt A, Droescher M, Knobeloch KP and Vinkemeier U: SUMO conjugation of STAT1 protects cells from hyperresponsiveness to IFNγ. Blood 118: 1002-1007, 2011.
28. Ma Y, Yan R, Wan Q, Lv B, Yang Y, Lv T and Xin W: Inhibitor of growth 2 regulates the high glucose-induced cell cycle arrest and epithelial-to-mesenchymal transition in renal proximal tubular cells. J Physiol Biochem 76: 373-382, 2020.
29. Sun YB, Qu X, Caruana G and Li J: The origin of renal fibroblasts/myofibroblasts and the signals that trigger fibrosis. Differentiation 92: 102-107, 2016.
30. Wang B, Ding W, Zhang M, Li H and Gu Y: Rapamycin attenuates aldosterone induced tubulointerstitial inflammation and fibrosis. Cell Physiol Biochem 35: 116-125, 2015.
31. Hu J, Zhu Q, Li PL, Wang W, Yi F and Li N: Stem cell conditioned culture media attenuated albumin-induced epithelial-mesenchymal transition in renal tubular cells. Cell Physion Biochem 35: 1719-1728, 2015.
32. Quaggin SE and Kapus A: Scar wars: Mapping the fate of epithelial-mesenchymal-myofibroblast transition. Kidney Int 80: 41-50, 2011.
33. Chatterjee-Kishore M, Wright KL, Ting JP and Stark GR: How Stat1 mediates constitutive gene expression: A complex of unphosphorylated Stat1 and IRF1 supports transcription of the LMP2 gene. EMBO J 19: 4111-4122, 2000.
34. Rodriguez MS, Dargemont C and Hay RT: SUMO-1 conjugation in vivo requires both a consensus modification motif and nuclear targeting. J Biol Chem 276: 12654-12659, 2001.
35. Jiang Y, Yu M, Hu X, Han L, Yang K, Ba H, Zhang Z, Yin B, Yang XP, Li Z and Wang J: STAT1 mediates transmembrane TNF-alpha-induced formation of death-inducing signaling complex and apoptotic signaling via TNFR1. Cell Death Differ 24: 660-671, 2017.